

Simulating fouling impact on the permeate flux in high-pressure membranes



Hisham A. Maddah*

Department of Chemical Engineering, King Abdulaziz University, Rabigh, Saudi Arabia

ARTICLE INFO

Article history:

Received 31 January 2021

Received in revised form

16 April 2021

Accepted 20 April 2021

Keywords:

Membrane separation

Desalination

FFD fouling simulation

Reverse osmosis

ABSTRACT

Porous high-pressure membranes have been widely used for saline water desalination. However, fouling (concentration polarization) extensively reduces permeate flux in reverse osmosis (RO) and/or nanofiltration (NF) modules. Fouling arises from pore blocking, organic adsorption, cake formation, inorganic or biological precipitation reducing water flux. Herein, we investigated the effect of feed water with various NaCl concentrations on fouling of RO and/or NF and the permeate water flux. A parabolic (or diffusion) partial differential equation (PDE) was used to model salt concentration profile or gradient inside the membrane. Subsequently, the numerical PDE equation, solved by the forward finite difference (FFD) explicit method, estimated flux decline rates resulted from NaCl fouling. It was found that salt accumulation occurs at the feed-side with a noticeable decrease in flux as fouling increases. Previous works reported similar findings as those identified from our analysis: (1) fouling increases with feed concentration and surface roughness, (2) fouling becomes intensified with higher pressure and flux, (3) fouling from long operation times can reduce flux by 65% within 24 h, (4) NaCl fouling can decrease flux rates by 70% (67-22 LMH) for brackish water with an initial concentration of 10000 ppm, and (5) reversible organic fouling may be avoided from lowering flux rates below the membrane critical flux. Results showed fouled RO modules would decrease flux rates from the increased surface polarization, where reverse flow (negative flux) was estimated for feed-side accumulations >10000 ppm for waters with an initial NaCl concentration of 10000 ppm and average diffusivity of $1.3 \times 10^{-6} \text{ cm}^2/\text{s}$.

© 2021 The Authors. Published by IASE. This is an open access article under the CC BY-NC-ND license (<http://creativecommons.org/licenses/by-nc-nd/4.0/>).

1. Introduction

Life qualities of human beings are totally dependent upon the possibility of meeting vast communities' demands on drinking water which is prioritized as a top necessity for people (Ogbonmwan, 2011; Maddah and Alzhrani, 2017). Water desalination through reverse osmosis (RO) and nanofiltration (NF) membranes remains the most commonly used separation process in comparison to other conventional desalination technologies such as multi-effect distillation (MED), multi-stage flash (MSF), and electrodialysis (ED), for the production of freshwater (Alawadhi, 2002; Bruggen and Vandecasteele, 2002; Maddah et al.,

2018). However, RO and NF membranes require a high-pressure operation for seawater desalination where fouling issues will inevitably arise on membrane surface due to impurities accumulation and micro-particles/organics precipitation on the membrane permeate-side (Bruggen and Vandecasteele, 2002; Maddah et al., 2017; Maddah et al., 2018). Drioli et al. (2002) suggested that having a pretreatment system (e.g., microfiltration and/or ultrafiltration) prior to RO and NF modules would certainly mitigate fouling issues and extend membrane lifetime for several years. According to Rajamohan et al. (2014), RO membranes are very susceptible to organic compounds; hence, biofouling problems arising from the removal of total organic carbon (TOC) and trihalomethane (THM) from contaminated water are more damaging to RO membranes than the conventional fouling issues from metallic and/or salt ions.

Typically, membranes separate contaminants from water by passing them through tubular polymer films that will capture impurities on the

* Corresponding Author.

Email Address: hmaddah@kau.edu.sa<https://doi.org/10.21833/ijaas.2021.08.001>

Corresponding author's ORCID profile:

<https://orcid.org/0000-0002-8208-8629>

2313-626X/© 2021 The Authors. Published by IASE.

This is an open access article under the CC BY-NC-ND license

[\(http://creativecommons.org/licenses/by-nc-nd/4.0/\)](http://creativecommons.org/licenses/by-nc-nd/4.0/)

retentate side (Maddah, 2016b; Maddah et al., 2017). Fouling takes place when dissolved and particulate matter in the feed water gets deposited on the membrane surface-side resulting in increasing membrane resistance to the feed flow (Aleem et al., 1998). Theoretically, membrane fouling can be categorized into four different types based on the feedwater constitutes as the following: (1) scale (inorganic); (2) particulate; (3) biological and (4) organic compounds (Qureshi et al., 2013).

Fouling consequences on membrane systems, particularly on RO and NF modules, are as the following: (1) flux decline and salt passage due to the developed concentration polarization; (2) film degradation and damage from the increased differential/feed pressure; (3) energy loss and poor operation owing to high-pressure and frequent cleaning requirements; (4) treatment cost increase; and (5) permeate quality reduction (Flemming, 1997; Aleem et al., 1998; Baker and Dudley, 1998). Accordingly, addressing fouling issues in RO/NF membranes through modeling and numerical analysis (Maddah, 2016d; 2016a; 2018a; 2018b; 2019a; 2018c; 2019b; Maddah et al., 2020a; 2020b) might be a fruitful way of understanding fouling behavior for better protection. In this work, we investigate the effect of NaCl salts on fouling of RO and/or NF membranes due to the treatment of saltwater with different concentrations. Feed waters with various initial concentrations (NaCl) of 10000 ppm (mimicking desalination of groundwater or brackish water) with a chosen fouling concentration range of 0–20000 ppm were studied. Numerical analysis was carried using the forward finite difference (FFD) explicit method along with other assumptions to calculate the decline in the flux rates and correlate the observed flux declines to the selected fouling concentrations.

2. Study assumptions and model parameters

2.1. Study assumptions

The effect of membrane fouling was studied in high-pressure membranes which were RO and/or NF with assumptions from previous works (Lonsdale et al., 1965; Al-Hobaib et al., 2015): (1) NaCl rejections of RO and NF are 95% and 50%, respectively (Maddah and Chogle, 2017; Maddah, 2020a; 2020b); (2) initial salt (NaCl) concentration is 10000 ppm; (3) water has an average membrane diffusivity of $1.3 \times 10^{-6} \text{ cm}^2/\text{s}$; and (4) membrane feed-side surface (fouling) concentrations are in the range 0–20000 ppm. Involved study parameters and their selected values which were used in the FFD numerical analysis are shown in Table 1.

2.2. Model parameters

RO membrane configuration (spiral-wound module) is shown in Fig. 1. Raw water enters the membrane through the module shell-side by

applying a high pressure that is enough to push water spirally along the feed spacers enveloping a long-rolled thin film composite (TFC) film which can retain undesired salts and ions. Freshwater is collected from the permeate output (tube-side) owing to the spiral-wound TFC film that would only allow fresh water to pass through diffusion while excluding other contaminants (concentrate output on the shell-side).

Table 1: FFD model parameters and their selected values

Parameter (Symbol)	Value	Unit
Rejection (R); for RO and NF*	95 and 50, respectively	%
Initial salt concentration (C_0)*	10000	ppm
Fouling concentration (C_f)*	0 ~ 20000	ppm
Water diffusivity (D)	1.3×10^{-6}	$\text{cm}^2 \text{ s}^{-1}$
Membrane thickness ($z = L$)	250	μm
Treatment/passing time (t)	25	s

*for brackish water with sodium chloride salts (NaCl) only

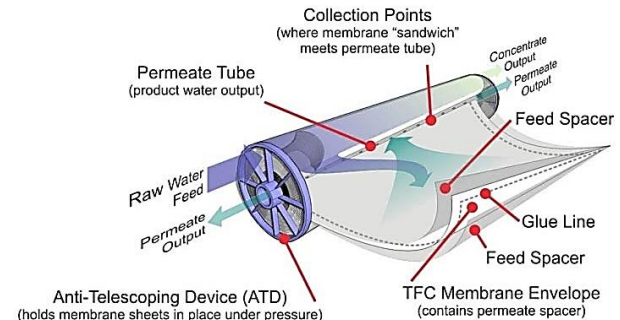


Fig. 1: Spiral-wound RO membrane configuration; Adapted from (AXEON, 2015)

3. Method and equations

For the FFD numerical analysis, the parabolic (or diffusion) partial differential equation (PDE) from (1) has been used along with the application of the FFD method (explicit) to get (2); where notations referring to space and time are as the following: $\{(i, k) = (z, t)\}$. FFD is a powerful mathematical method used to convert PDEs, such that (1), to equations in the algebraic form to be solved numerically. By using the converted and analytically determined equation, as shown in (2), we have been capable of estimating the salt concentration profile within the membrane (equations were solved through a programmed algorithm code in MATLAB) (Deen, 2011; Chapra and Canale, 2015; Maddah, 2016c).

$$\frac{\partial c}{\partial t} = D \frac{\partial^2 c}{\partial z^2} \quad (1)$$

$$C_i^{k+1} = C_i^k + \frac{D \Delta t}{(\Delta z)^2} (C_{i+1}^k - 2C_i^k + C_{i-1}^k) \quad (2)$$

For further analysis, total water flux across the RO and/or NF membrane was determined from Fick's first law (Deen, 2011) as shown in (3) and at the selected fouling concentrations which were previously reported in Table 1. Initial, fouling, and total flux rates were calculated from both (4) and (5).

$$J = -D \frac{dC}{dz} = -D \left[\frac{C - C_0}{z - z_0} \right] \quad (3)$$

$$J_0 = -D \left[\frac{C_P - C_0}{L} \right] ; J_f = -D \left[\frac{C_f - C_0}{L} \right] \quad (4)$$

$$J_T = J_0 - (J_0 - J_f) \quad (5)$$

where J is the flux rate ($\text{g cm}^{-2} \text{s}^{-1}$); subscripts: 0, P , f and T refer to initial, permeate, fouling, and total, respectively, D is water diffusivity into the membrane ($\text{cm}^2 \text{s}^{-1}$), C is salt concentration in (g cm^{-3}) and z refers to the spatial position (cm) with respect to membrane thickness, L .

Based on RO and/or NF membrane structure described in previous works (AUXIAQUA, 2011; Al-Hobaib et al., 2015), we have only considered the polyamide (PA) layer for the flux calculations, and that fouling layer was assumed to only occur in the PA layer. The PA layer was selected instead of the other layers (PSF and PEST from Fig. 2 and Table 2) because PA has a very small pore size as compared to the other layers making our selection a valid approximated assumption. The very small pore size in PA makes it responsible for the high membrane rejection and flow resistance in both RO and/or NF membranes. Hence, membrane resistance to water flow from PSF and PEST layers can be neglected due to their larger pores which allow easy water flow with minimal back pressure (despite that PSF and PEST are much thicker than PA, their resistances are still negligible due to the larger pores which are three orders of magnitude higher than PA pores).

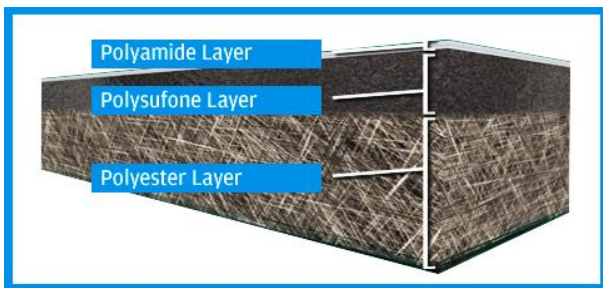


Fig. 2: Membrane layer structure (AUXIAQUA, 2011)

Table 2: RO/NF Membrane layers and their thickness

Membrane Layer	Selected	Literature
Polyamide (PA)*	62.5 nm	1–200 nm
Polysulfone (PSF)	40 μm	30–50 μm
Polyester (PEST)	150 μm	100–200 μm

*Flux rates were calculated based on the PA layer only; since the resistance of other layers were neglected due to their larger pores (much larger pore diameters as compared to PA)

4. Results and discussion

Dimensionless concentration profiles of NaCl salts within the treated water inside the membrane are shown in Fig. 3 with respect to both membrane treatment time (time) and membrane thickness (space) at various selected fouling concentrations. Salt accumulations (NaCl) on the membrane surface were observed to occur much frequently at high fouling concentrations; there should be proportionality between feed salt concentration and membrane fouling rates. High fouling rates resulted in lowering membrane treatment efficiency across

the membrane thickness due to the high amounts of NaCl salts accumulated onto the surface which extensively reduced the ideal treatment condition of ~ 0 ppm salts in the produced water (indicated as blue regions in Fig. 3). As expected, the best instantaneous treatment efficiency was determined when $C_f = 0$; and there was a noticeable decrease in the instantaneous efficiency with the build-up fouling ($C_f > 0$ ppm) with the worst treatment performance when fouling was furtherly progressed ($C_f \rightarrow 2C_0$). In other words, the permeation may get highly contaminated at high fouling rates owing to extensive salt accumulations on the membrane surface and within membrane film (thickness). Typically, membrane cleaning may only help in the removal of salts accumulated on the surfaces (as $C_f < 1000$ ppm); but as fouling progress to higher levels (as $C_f > 7000$ ppm), membrane cleaning would become more difficult due to arising of inner-membrane fouling besides the surface fouling which might make it more difficult to flush out trapped salt ions to achieve better instantaneous membrane performance.

The impact of membrane fouling and concentration polarization (surface and inner) on the permeate flux rates (feed water across the membrane) is shown in Fig. 4. Since we have selected a fixed initial salt concentration, forward water fluxes (J_0) at initial treatment times were found to be constant across the membrane regardless of C_f value. However, backward fluxes at membrane surface were found to be linearly intensified with fouling rates (high C_f yield in shifting backward flux values from positive to negative; indicating that fouled membranes progress high surface resistance to water flow which might reverse water direction in severe cases). Thus, reduced water flux defined as ($J_0 - J_f$) has been expected to behave with an almost opposite behavior to J_f in which reduced water flux positively and linearly increases with the increase in fouling concentrations. Total flux rates observed across the membrane have been clearly identified to be linearly decreasing (from 74.9 to 0 LMH) with the increase in the assigned fouling concentrations ($C_f \rightarrow C_0$) owing to the high amounts of accumulated salts explained via reduced flux rates; when $C_f > C_0$, membrane would be in the worst-case scenario where most of the pores will be clogged from concentration polarization, hence, total water flux rates could be reversed across the membrane where negative flux indicates a back-flow scenario (as illustrated in Fig. 4).

5. Comparative analysis and outlook

According to Guo et al. (2012), various membrane fouling mechanisms include concentration polarization, pore blocking, organic adsorption, cake formation, inorganic precipitation, and/or biological fouling, which are all unfavorable phenomena when

it comes to the application of membrane separation for water and wastewater treatment. Understanding foulant interactions with membrane surface charge is the key to solve such fouling problems that would reduce permeate flux rates, increase pressure, and reduce productivity. Thus, developing a proper pretreatment method allows overcoming fouling issues for increased membrane lifetime with less maintenance and operation costs (Guo et al., 2012; Maddah and Chogle, 2015; Maddah, 2016a; 2019a; 2019b).

In terms of composite polyamide RO membranes, colloidal fouling rates from Silica colloids have been

found to increase drastically with the increase in feed concentration and permeate water flux, as suggested in this study from NaCl concentration polarization.

Moreover, solution ionic strength was determined to be a controlling factor that tunes fouling rates based on the "interplay between permeation drag and electric double layer repulsion" and precisely from the relationship between physical and chemical interactions, knowing that surface roughness is not favored to reduce fouling mechanisms (Zhu and Elimelech, 1997).

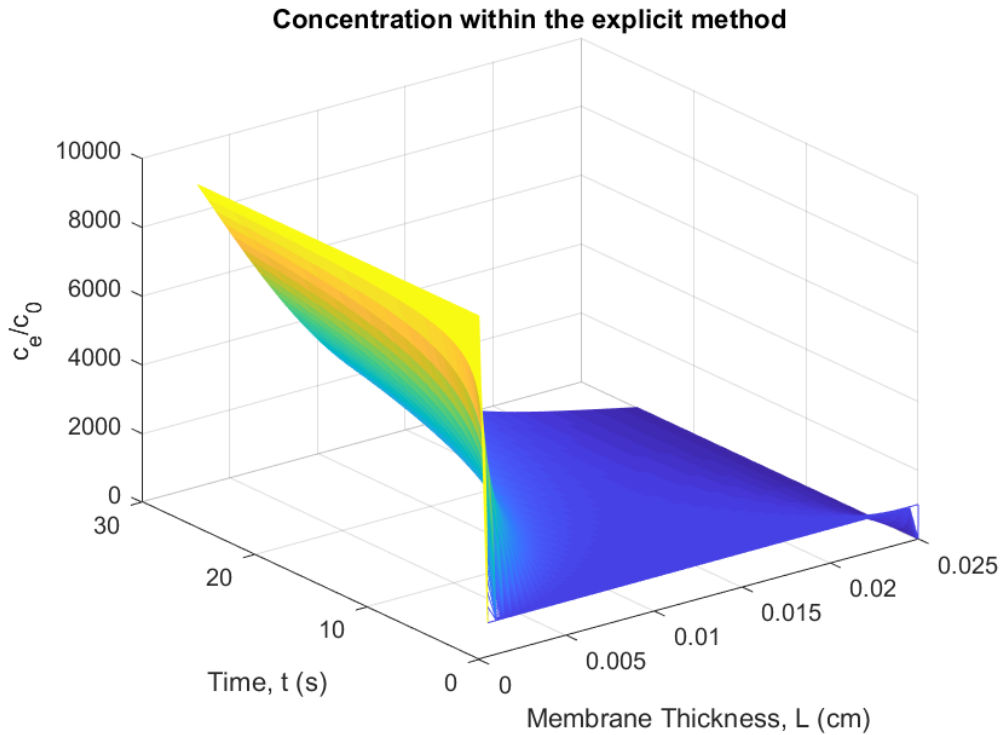
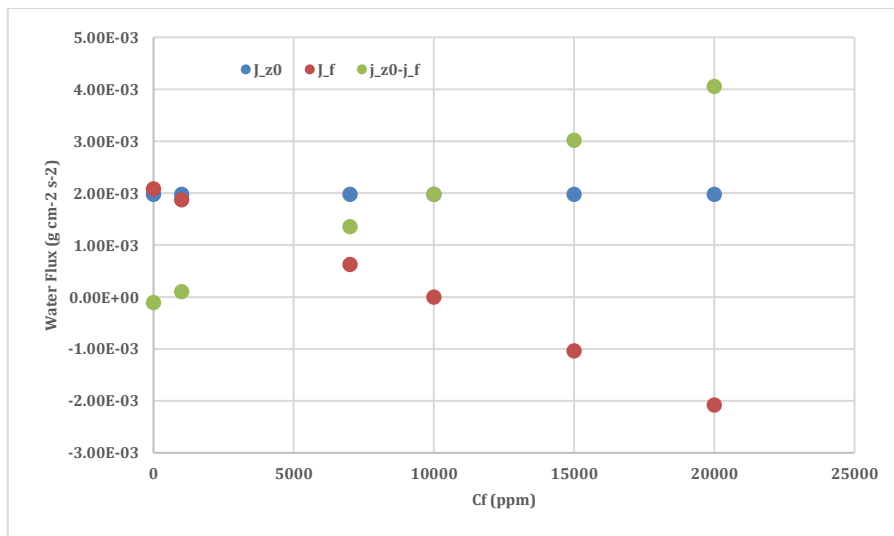


Fig. 3: Salt concentration profile as a function of membrane treatment time and thickness at an initial concentration (C_0) of 10000 ppm and different fouling concentrations (C_f)



a

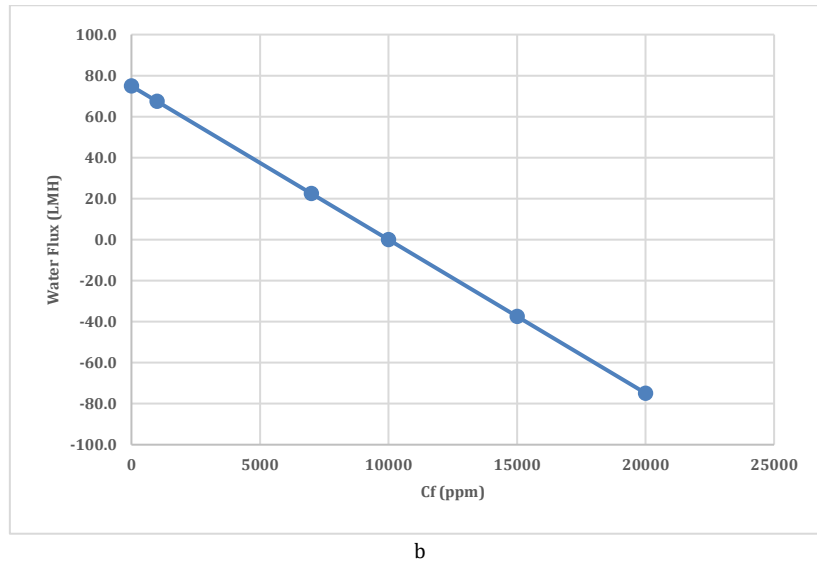


Fig. 4: Observed water flux across the membrane at an initial concentration (C_0) of 10000 ppm and at different fouling concentrations (C_f): (a) Forward, backward, and reduced fluxes; (b) Total flux: $J_T = J_0 - (J_0 - J_f)$

Li et al. (2007) found that RO membranes develop faster fouling with higher initial permeate flux or applied pressure resulting from enhanced fouling layer compression and foulants deposition rates. Fouling rates from both bovine serum albumin (BSA) and sodium alginate biopolymers were investigated to show that alginate fouled RO membranes much faster than BSA in the presence of calcium divalent cations. Very high operating pressure negatively impact membrane performance and surface properties (e.g. smoothness, zeta potential, and hydrophobicity) from compounded fouling of multiple existing foulants (Li et al., 2007).

A critical-flux concept has been earlier established for low-pressure and high-pressure microfiltration membranes, which states that "on start-up, there exists a flux below which a decline of flux with time does not occur". Over-fouling might be avoided by constant flux filtration techniques with moderate-to-high transmembrane pressure, where it is desired to start the filtration at a low flux rate before reaching the critical-flux for minimum fouling and consistent flux rates (Field et al., 1995). Fouling resistance of brackish water (Maddah and Shihon, 2018) membranes can be improved by surface modification via incorporating graphene oxide to directly coat a GO/f-Cs thin layer on the membrane surface, as experimented by Hegab et al. (2015). Surface characterization studies for the modified GO/f-Cs/PA composite membranes showed increased membrane hydrophilicity, smoothness, water flux, and NaCl rejection rates. Such improvements in membrane performance of the modified membranes were possible due to the enhanced antifouling property (improved organic fouling resistance), which resulted in less flux decline and a much higher water recovery ratio (97%). An increase of 20% in permeation flux rates has been observed for modified membranes used in the treatment of a feed solution containing 1500 ppm of NaCl under 14 bar, with a salt rejection of 95.6%. Thus, the creation of thin active layers of

GO/f-Cs on membrane surfaces proved to enhance water permeability because of amphiphilic GO and hydrophilic Cs (Hegab et al., 2015).

Regarding the fouling control in forward osmosis (FO) membranes, Boo et al. (2013) suggested efficient hydrodynamic strategies such as using a feed-channel spacer or pulse flow during osmotic dilution. Such strategies like this can mitigate fouling rates by loosening the built-up inorganic/organic fouling layer for higher permeate water flux rates. However, higher flux rates over long operation times cause increased concentration polarization from particulate and organic matter found in saline water (Boo et al., 2013).

Based on a fouling propensity study on FO membranes, it has been hypothesized that FO shows a slower flux decline correlated with the lower observed fouling rates. This hypothesis has been proved by an experimental and theoretical approach where the slower flux decline phenomenon is due to (1) much smoother and dense membrane surfaces, and (2) lower internal concentration polarization in FO, than that the conventional high-pressure driven membranes, thereby, producing higher water quality at lower energy consumption rates. In FO, natural osmotic pressure is the driving force that would draw pure water from a feed flow *via* utilizing a concentrated draw solution (Lay et al., 2010). FO membranes operated below the critical flux would cause reversible organic fouling which can be overcome by having an optimal flux of 21-25 LMH for long-term operations for wastewater reclamation. Cake layer (irreversible fouling) on top of membrane surfaces may form with >30-35 LMH, from single or multiple foulants with 60 mg/L concentration, decreases membrane practicability and performance (Nguyen et al., 2020).

A previous case study on the treatment of non-chlorinated brackish lake water via FO suggests that biological fouling progression (exponentially) develops over time and during the experimental period. Both organic (microbial) fouling and

biofouling (bacterial) (Maddah and Chogle, 2017) were observed to occur from protein-like substances. The water flux was found to decline by approximately 65% of the initial value after the 24 h fouling experiments. However, flux reversibility to its initial level was possible with membrane surface hydraulic cleaning by deionized water (Chun et al., 2015). According to She et al. (2012) FO membrane fouling by alginate can significantly impact water flux rates based on the selected draw solution. It has been shown that the greatest reverse solute diffusion rate was observed for NaCl among the four studied types of draw solution of NaCl, MgCl₂, CaCl₂ and Ca(NO₃)₂, which was consistent with the solute permeability coefficients. Promoted forward feed

solutes diffusion caused by increased concentration polarization (fouling) can be avoided by selecting a proper draw solution (cation and anion type) that does not contain undesired divalent organic fouling initiators. Moreover, using a membrane with high selectivity is a good strategy to control fouling from NaCl draw solution in FO, and reduce pore-clogging (concentration polarization) and rate of forward diffusion of Na⁺ in the feed solution for better water flux rates (She et al., 2012). Table 3 shows a thorough evaluation of our results and analysis from comparisons of the impact of membrane fouling based on similar previous studies remarks and results obtained from fouling experiments on RO, FO, or RO/FO modules.

Table 3: Results evaluation and analysis of the fouling impact on the permeate flux in RO and FO membranes from comparisons with similar previous studies observations

Membrane	Remarks and Observations from Fouling Impact	Ref.
RO/FO	Fouling arises from pore blocking, organic adsorption, cake formation, inorganic or biological precipitation reducing water flux.	(Guo et al., 2012)
RO	Colloidal fouling from Silica colloids increases drastically with the increase in feed concentration, permeate flux, and surface roughness.	(Zhu and Elimelech, 1997)
RO	Fouling increases with higher initial permeate flux or pressure from both bovine serum albumin (BSA) and sodium alginate.	(Li et al., 2007)
RO	Surface modification <i>via</i> GO/f-Cs increases antifouling, hydrophilicity, smoothness, and flux by 20% of 1500 ppm NaCl, 14 bar.	(Hegab et al., 2015)
FO	Higher flux rates over long operation times increase fouling from particulate and organic matter found in saline water.	(Boo et al., 2013)
FO	Slower flux decline occurs in smoother and dense membranes.	(Lay et al., 2010)
FO	Operation below critical flux cause reversible organic fouling avoidable with a flux of 21-25 LMH. Cake layer (irreversible fouling) occurs >30-35 LMH, from foulants with 60 mg/L concentration.	(Nguyen et al., 2020)
FO	Biological fouling exponentially develops over time reducing initial flux by 65% within 24 h. High selectivity to control NaCl fouling, which showed the greatest reverse solute diffusion rate.	(She et al., 2012)
RO	Salt accumulation occurs at the membrane feed-side decreasing flux rates by 10-70% (22-67 LMH) of 10000 ppm NaCl. Reverse flow (negative flux) was estimated for membrane surface with accumulations >10000 ppm.	This Study

6. Conclusion

Fouling (concentration polarization) associated with brackish water and seawater desalination in high-pressure membranes (RO/NF) was studied numerically to determine fouling impact on salt concentration profile and permeate flux rates of treated water. PDE equations were solved analytically through the FFD method and then coded in MATLAB for carrying out the results. Salt accumulations at the membrane feed-side surface were found to increase with fouling concentration which would decrease membrane treatment efficiency. In comparison with earlier studies, similar findings were experimentally identified when using RO or FO modules, including that fouling increases with feed concentration, surface roughness, applied pressure, water flux, operation times, and from reaching the membrane critical flux rate. Our numerical analysis revealed that high fouling would lower water flux due to undesired salt accumulations ($J_T = 0$ at $C_f = C_0$; and backflow at $C_f > C_0$). Total flux rates linearly decreased (from 74.9 to 0 LMH) with the increase in the assigned fouling concentrations ($C_f \rightarrow C_0$). When $C_f > C_0$, RO membranes would be in the worst-case scenario where most of the pores will be clogged, hence, total water flux rates could be reversed. In other words,

fouled RO modules would decrease flux rates from the increased surface polarization, where reverse flow (negative flux) was estimated for feed-side accumulations >10000 ppm for waters with an initial NaCl concentration of 10000 ppm and average diffusivity of 1.3×10^{-6} cm²/s. Membrane cleaning may only help in the removal of salts accumulated on the surfaces (as $C_f < 1000$ ppm); but as fouling progress to higher levels (as $C_f > 7000$ ppm), membrane cleaning would become more difficult due to arising of inner-membrane fouling besides the surface fouling. Moreover, NaCl fouling can decrease flux rates by 70% (22-67 LMH) from brackish water treatment, where flux may further decline with long operation times >24 h. It has been concluded that fouling can severely damage RO modules from high salt accumulations decreasing membrane treatment efficiency due to lowered permeate flux. Future works may focus on increasing membrane antifouling capability by enhancing membrane surface hydrophilicity and smoothness *via* surface modification for improved flux, operation, and overall brackish water desalination performance.

Acknowledgment

The author gratefully appreciates the support provided by the Deanship of Scientific Research at

King Abdulaziz University which facilitated the completion of this work.

Compliance with ethical standards

Conflict of interest

The author(s) declared no potential conflicts of interest with respect to the research, authorship, and/or publication of this article.

References

- Alawadhi AA (2002). Regional report on desalination-GCC countries. In the IDA World Congress on Desalination and Water Reuse, Manama, Bahrain: 8-13.
- Aleem AEFA, Al-Sugair KA, and Alahmad MI (1998). Biofouling problems in membrane processes for water desalination and reuse in Saudi Arabia. *International Biodeterioration and Biodegradation*, 41(1): 19-23. [https://doi.org/10.1016/S0964-8305\(98\)80004-8](https://doi.org/10.1016/S0964-8305(98)80004-8)
- Al-Hobaib AS, Al-Sheetan KM, Shaik MR, Al-Andis NM, and Al-Suhybani MS (2015). Characterization and evaluation of reverse osmosis membranes modified with Ag₂O nanoparticles to improve performance. *Nanoscale Research Letters*, 10(1): 1-13. <https://doi.org/10.1186/s11671-015-1080-3> **PMid:26428014** **PMCID:PMC4883278**
- AUXIAQUA (2011). Filtration systems: Reverse osmosis. Available online at: <http://www.auxiaqua.es/en/sistemas-filtracion/>
- AXEON (2015). Reverse osmosis membrane element construction. AXEON Water Technologies, Temecula, USA.
- Baker JS and Dudley LY (1998). Biofouling in membrane systems: A review. *Desalination*, 118(1-3): 81-89. [https://doi.org/10.1016/S0011-9164\(98\)00091-5](https://doi.org/10.1016/S0011-9164(98)00091-5)
- Boo C, Elimelech M, and Hong S (2013). Fouling control in a forward osmosis process integrating seawater desalination and wastewater reclamation. *Journal of Membrane Science*, 444: 148-156. <https://doi.org/10.1016/j.memsci.2013.05.004>
- Bruggen BV and Vandecasteele C (2002). Distillation vs. membrane filtration: Overview of process evolutions in seawater desalination. *Desalination*, 143(3): 207-218. [https://doi.org/10.1016/S0011-9164\(02\)00259-X](https://doi.org/10.1016/S0011-9164(02)00259-X)
- Chapra SC and Canale RP (2015). Numerical methods for engineers. McGraw-Hill, New York, USA.
- Chun Y, Zaviska F, Cornelissen E, and Zou L (2015). A case study of fouling development and flux reversibility of treating actual lake water by forward osmosis process. *Desalination*, 357: 55-64. <https://doi.org/10.1016/j.desal.2014.11.009>
- Deen WM (2011). Analysis of transport phenomena. 2nd Edition, DEEN Publisher, London, UK.
- Drioli E, Criscuoli A, and Curcio E (2002). Integrated membrane operations for seawater desalination. *Desalination*, 147(1-3): 77-81. [https://doi.org/10.1016/S0011-9164\(02\)00579-9](https://doi.org/10.1016/S0011-9164(02)00579-9)
- Field RW, Wu D, Howell JA, and Gupta BBJ (1995). Critical flux concept for microfiltration fouling member. *Journal of Membrane Science*, 100(3): 259-272. [https://doi.org/10.1016/0376-7388\(94\)00265-Z](https://doi.org/10.1016/0376-7388(94)00265-Z)
- Flemming HC (1997). Reverse osmosis membrane biofouling. *Experimental Thermal and Fluid Science*, 14(4): 382-391. [https://doi.org/10.1016/S0894-1777\(96\)00140-9](https://doi.org/10.1016/S0894-1777(96)00140-9)
- Guo W, Ngo HH, and Li J (2012). A mini-review on membrane fouling. *Bioresource Technology*, 122: 27-34. <https://doi.org/10.1016/j.biortech.2012.04.089> **PMid:22608938**
- Hegab HM, Wimalasiri Y, Ginic-Markovic M, and Zou L (2015). Improving the fouling resistance of brackish water membranes via surface modification with graphene oxide functionalized chitosan. *Desalination*, 365: 99-107. <https://doi.org/10.1016/j.desal.2015.02.029>
- Lay WC, Chong TH, Tang CY, Fane AG, Zhang J, and Liu Y (2010). Fouling propensity of forward osmosis: Investigation of the slower flux decline phenomenon. *Water Science and Technology*, 61(4): 927-936. <https://doi.org/10.2166/wst.2010.835> **PMid:20182071**
- Li Q, Xu Z, and Pinnau I (2007). Fouling of reverse osmosis membranes by biopolymers in wastewater secondary effluent: Role of membrane surface properties and initial permeate flux. *Journal of Membrane Science*, 290(1-2): 173-181. <https://doi.org/10.1016/j.memsci.2006.12.027>
- Lonsdale HK, Merten U, and Riley RL (1965). Transport properties of cellulose acetate osmotic membranes. *Journal of Applied Polymer Science*, 9(4): 1341-1362. <https://doi.org/10.1002/app.1965.070090413>
- Maddah HA (2016a). Optimal operating conditions in designing photocatalytic reactor for removal of phenol from wastewater. *ARPN Journal of Engineering and Applied Sciences*, 11(3): 1799-1802.
- Maddah HA (2016b). Polypropylene as a promising plastic: A review. *American Journal of Polymer Science*, 6(1): 1-11.
- Maddah HA (2016c). Application of finite Fourier transform and similarity approach in a binary system of the diffusion of water in a polymer. *Journal of Materials Science and Chemical Engineering*, 4(4): 20-30. <https://doi.org/10.4236/msce.2016.44003>
- Maddah HA (2016d). Modeling the relation between carbon dioxide emissions and sea level rise for the determination of future (2100) sea level. *American Journal of Environmental Engineering*, 6(2): 52-61.
- Maddah HA (2018a). Modeling the feasibility of employing solar energy for water distillation. In: Hussain CM (Ed.), *Handbook of environmental materials management*: 1-25. Springer, Cham, Switzerland. https://doi.org/10.1007/978-3-319-58538-3_120-1
- Maddah HA (2018b). Analytical derivation of diffusio-osmosis electric potential and velocity distribution of an electrolyte in a fine capillary slit. *International Journal of Engineering and Technology*, 18(3): 1-9.
- Maddah HA (2018c). Numerical analysis for the oxidation of phenol with TiO₂ in wastewater photocatalytic reactors. *Engineering, Technology and Applied Science Research*, 8(5): 3463-3469. <https://doi.org/10.48084/etasr.2304>
- Maddah HA (2019a). Industrial membrane processes for the removal of VOCs from water and wastewater. *International Journal of Engineering and Applied Sciences*, 6(4): 21-26. <https://doi.org/10.31873/IJEAS/6.4.2019.09>
- Maddah HA (2019b). Modeling and designing of a novel lab-scale passive solar still. *Journal of Engineering and Technological Sciences*, 51: 303-322. <https://doi.org/10.5614/j.eng.technol.sci.2019.51.3.1>
- Maddah HA (2020a). Adsorption isotherm of NaCl from aqueous solutions onto activated carbon cloth to enhance membrane filtration. *Journal of Applied Science and Engineering*, 23(1): 69-78.
- Maddah HA (2020b). Transport of electrolyte solutions along a plane by diffusion-osmosis. *ARPN Journal of Engineering and Applied Sciences*, 15: 46-51.
- Maddah HA and Alzhrani AS (2017). Quality monitoring of various local and imported brands of bottled drinking water in Saudi Arabia. *World Journal of Engineering and Technology*, 5(4): 551-563. <https://doi.org/10.4236/wjet.2017.54047>
- Maddah HA and Chogle A (2017). Biofouling in reverse osmosis: Phenomena, monitoring, controlling and remediation. *Applied*

- Water Science, 7(6): 2637-2651.
<https://doi.org/10.1007/s13201-016-0493-1>
- Maddah HA and Chogle AM (2015). Applicability of low pressure membranes for wastewater treatment with cost study analyses. *Membrane Water Treatment*, 6(6): 477-488.
<https://doi.org/10.12989/mwt.2015.6.6.477>
- Maddah HA and Shihon MA (2018). Activated carbon cloth for desalination of brackish water using capacitive deionization. In: Eyvaz M and Yüksel E (Eds.), *Desalination and Water Treatment: 17-36*. Books on Demand, Norderstedt, Germany.
<https://doi.org/10.5772/intechopen.76838>
- Maddah HA, Alzhrani AS, Almalki AM, Bassyouni M, Abdel-Aziz MH, Zoromba M, and Shihon MA (2017). Determination of the treatment efficiency of different commercial membrane modules for the treatment of groundwater. *Journal of Materials and Environmental Science*, 8(6): 2006-2012.
<https://doi.org/10.1007/s13201-018-0793-8>
- Maddah HA, Alzhrani AS, Bassyouni M, Abdel-Aziz MH, Zoromba M, and Almalki AM (2018). Evaluation of various membrane filtration modules for the treatment of seawater. *Applied Water Science*, 8(6): 1-13.
<https://doi.org/10.1007/s13201-018-0793-8>
- Maddah HA, Bassyouni M, Abdel-Aziz MH, Zoromba MS, and Al-Hossainy AF (2020a). Performance estimation of a mini-passive solar still via machine learning. *Renewable Energy*, 162: 489-503. <https://doi.org/10.1016/j.renene.2020.08.006>
- Maddah HA, Berry V, and Behura SK (2020b). Cuboctahedral stability in Titanium halide perovskites via machine learning. *Computational Materials Science*, 173: 109415.
<https://doi.org/10.1016/j.commatsci.2019.109415>
- Nguyen TT, Lee C, Field RW, and Kim IS (2020). Insight into organic fouling behavior in polyamide thin-film composite forward osmosis membrane: Critical flux and its impact on the economics of water reclamation. *Journal of Membrane Science*, 606: 118118.
<https://doi.org/10.1016/j.memsci.2020.118118>
- Ogbonmwan SE (2011). Water for life Ireland campaign: Supporting the united nation water campaign. The 2nd United Nation Water day, Expo, Trinity Science Gallery, Dublin, Ireland.
- Qureshi BA, Zubair SM, Sheikh AK, Bhujle A, and Dubowsky S (2013). Design and performance evaluation of reverse osmosis desalination systems: An emphasis on fouling modeling. *Applied Thermal Engineering*, 60(1-2): 208-217.
<https://doi.org/10.1016/j.applthermaleng.2013.06.058>
- Rajamohan R, Venugopalan VP, Debasis M, and Usha N (2014). Efficiency of reverse osmosis in removal of total organic carbon and trihalomethane from drinking water. *Research Journal of Chemistry and Environment*, 18: 1-6.
- She Q, Jin X, Li Q, and Tang CY (2012). Relating reverse and forward solute diffusion to membrane fouling in osmotically driven membrane processes. *Water Research*, 46(7): 2478-2486.
<https://doi.org/10.1016/j.watres.2012.02.024>
PMid:22386887
- Zhu X and Elimelech M (1997). Colloidal fouling of reverse osmosis membranes: Measurements and fouling mechanisms. *Environmental Science and Technology*, 31(12): 3654-3662.
<https://doi.org/10.1021/es970400v>